[Chem. Pharm. Bull. 21(2) 394—403 (1973)]

UDC 615.011.3.014

Studies on Flowability of Powder and Interparticle Cohesion

Kozo Kurihara and Izuo Ichikawa

Product Development Laboratories, Sankyo Co., Ltd.[1]

(Received September 13, 1972)

The angles of repose and the discharge-behavior from small holes under a slow agitation were studied on powders with particles of comparatively wide size ranges. Moreover, the shear-tests were done on these powders and from these data the interparticle cohesion at point of contact under zero compacting pressure was determined. The relations between this interparticle cohesion and the angle of repose or the discharge-behavior were determined. These results are summarized as follows.

1. The relation between the discharge-rate Q(ml/min) and the relative dimension of the orifice-area to the particle-area is represented by the following equation.

$$Q = a((\phi/dp)^2 - (\phi_0/dp)^2)$$

2. The relation between a and the reciprocal of $(\phi_0/dp)^2$) is roughly linear.

3. ϕ_0/dp increases monotonically with $kFo/\rho pdp^3$ and the relation between them is independent of the particle-shape.

4. The angle of repose increases linearly with $Fo/\rho pdp^3$ and the relation between them is dependent on the particle-shape and in the range of small $Fo/\rho pdp^3$ the angle of repose of the spherical particle is smaller than that of the irregular one.

5. The relation between the discharge-behavior and the angle of repose could be represented by the following equation.

$$\phi_0/dp = f(k(\theta-\theta_0)/\alpha)$$

Introduction

The angle of repose, the minimum orifice-diameter for discharge and the rate of discharge through orifices have been used to express the flowability of powder.[2] Only a few reports have been published on the relations between the flowability and the primary properties of powders.[3] No correlations, however, between them have been reported on the powders smaller than about 50 μ diameter. The cohesion-forces of powder-beds have been measured with shear-tests by several workers.[4] No correlations, however, have yet been established between the cohesion and the flowability of powders. Both the angle of repose and the rate of discharge through orifices have been used as the index of flowability but negative correlations have been suggested.[5]

We did some experiments on shear-tests and measured the angles of repose, the minimum orifice-diameters and the rates of discharge through orifices on powders with their sizes ranging from 12 μ to 600 μ. An interparticle cohesion at point of contact, corresponding to that in a powder pile formed naturally, was determined from the data of shear-tests. And the

1) Location: *Hiromachi, Shinagawa-ku, Tokyo.*

2) *a*) E. Nakajima, *Yakugaku Zasshi*, **81**, 717 (1962); *b*) M. Noda, C. Hayashi, M. Ito, S. Fukui, and S. Fujita, *Yakuzaigaku*, **20**, 50 (1960); *c*) K. Kurihara and H. Kuno, *J. Appl. Phys., Japan*, **34**, 727 (1965); *d*) G. Gold, R.N. Duvall, B.T. Palermo, and J.G. Slater, *J. Pharm. Sci.*, **57**, 2153 (1968).

3) *a*) O. Ohodaira, K. Okada, and H. Fujimoto, *J. Res. Assoc. Powder Tech.*, **8**, 237 (1971); *b*) M. Arakawa, T. Okada, and E. Suito, *Journal of the Society of Materials Science, Japan*, **15**, 151 (1966); *c*) F.Q. Danish and E.L. Parrott, *J. Pharm. Sci.*, **60**, 548 (1971).

4) *a*) E.N. Hiestand and C.J. Wilcox, *J. Pharm. Sci.*, **57**, 1421 (1968); *b*) J.C. Williams and A.H. Birks, *Powder Technol.*, **1**, 199 (1967).

5) *a*) G. Gold, R.N. Duvall, B.T. Palermo, and J.G. Slater, *J. Pharm. Sci.*, **55**, 1291 (1966); *b*) E.D. Sumner, H.O. Thompson, W.K. Poole, and J.E. Grizzle, *J. Pharm. Sci.*, **55**, 1441 (1966).

relationship of this interparticle cohesion with the angle of repose and the minimum orifice-diameter were studied. As the results of these studies, the interrelations were found among the interparticle cohesion, the angle of repose, the minimum orifice-diameter and the discharge-rate.

Experimental

The storage of samples and all experiments were done under the conditions of 23±1° and 70±3% RH in an air-conditioned room.

Materials——The particle-diameter, -shape and -density(ρ_p), the apparent bulk density(ρ_a) and the loss on drying are shown for all samples in Table I. No. 1,3,12,15 and 17 were purchased and used without treatment, and No. 2,4,16 and 18 were the mixture of magnesium stearate with each of No. 1,3,12 and 17, respectively. The concentration of magnesium stearate was 0.5%. No. 5, 6 and 7 were prepared by screening of No. 3 with the sieves shown in Table I, and No. 8,9,10 and 11 were prepared in the same way from microcrystalline cellulose. No. 13 and 14 were made in the following steps; the mixture of No. 1 and 11 in a 1:1 weight ratio was granulated with water by using a kneader and a Tornado-Mill and then, the granule was dried for 1 hr at 60° in an air-through dryer and screened with the sieves shown in Table I. No. 19 was cleaned in the following way and then used; it was treated at 80° for 5 hr in 5% Extra-flüssig (by Merck) aqueous solution and, after being washed with water several times, dried at 105° for 9 hr. No. 20 was made of thiamine mononitrate and wax by using a spray-dryer.

The average diameter(dp) shown in Table I is the Green diameter and determined from the measurements for 500 particles with a microscope. The particle-density (ρ_p) was measured with a mercury-picnometer for No. 13 and 14, and with Beckman Air-Comparison Picnometer for the other samples. The apparent bulk density (ρ_a) was determined in the following way; powder poured gently through a funnel into a hollow cylinder placed in a 100 ml Glass Cylindrical Graduate, and then, after the removal of the hollow cylinder from the Glass Cylindrical Graduate, the volume of the powder in the Glass Cylindrical Graduate was read with its scale (the amount of powder was predetermined so that its volume would be 95 to 100 ml), while the weight of the powder was determined from those of the Glass Cylindrical Graduate in the absence of and presence of the powder. ρ_a was calculated from the weight and the volume of the powder. The measurements were done 5 times and the deviations of individual ρ_a form the average were within ±5%. The average is shown in Table I. The loss on drying for 50 min at 80° was determined.

Table I. Materials Tested

Sample No.	Substance	Particle size ($\times 10^{-4}$ cm) dp	range	Density (g/cm³) ρ_p	ρ_a	Particle shape	Loss on drying (%)
1	lactose	12	5—20	1.53	0.53	irreg.	0.3
2	No. 1+Mg-St[a]	12	5—20	1.53	0.63	irreg.	0.1
3	lactose, cryst.	41	15—90	1.53	0.69	irreg.	0.3
4	No. 3+Mg-St	41	15—90	1.53	0.85	irreg.	0.1
5	lactose, cryst., −100/+150	127	105—150	1.53	0.74	irreg.	0.4
6	lactose, cryst., −150/+200	90	75—105	1.53	0.73	irreg.	0.2
7	lactose, cryst., −200/+250	65	60—75	1.53	0.72	irreg.	0.3
8	cryst. cellulose, −100/+150	127	105—150	1.55	0.25	irreg., rod-like	4.6
9	cryst. cellulose, −150/+200	90	75—105	1.55	0.26	irreg., rod-like	5.0
10	cryst. cellulose, −200/+250	68	60—75	1.55	0.27	irreg., rod-like	4.3
11	cryst. cellulose, −250/+300	55	47—60	1.55	0.29	irreg., rod-like	4.4
12	BTMP[b]	50	20—100	1.44	0.60	irreg.	0.8
13	No. 1+No. 11[c], −20/+35	600	420—850	1.09	0.48	irreg.	2.4
14	No. 1+No. 11, −100/+150	127	105—150	1.11	0.47	irreg.	3.4
15	corn starch	13	5—20	1.50	0.50	nearly spherical	4.2
16	No. 15+Mg-St	13	5—20	1.50	0.60	nearly spherical	4.0
17	potato starch	23	5—40	1.50	0.79	nearly spherical	3.5
18	No. 17+Mg-St	23	5—40	1.50	0.92	nearly spherical	3.5
19	glass beads	50	30—70	2.42	1.41	spherical	0.1
20	VB_1HNO_3[d]	64	15—80	1.10	0.35	spherical	0.3

a) magnesium stearate *b*) benzoyl thiamine monophosphate *c*) granulated *d*) spray-dried with wax

Apparatus and Method——An angle of repose was measured with the appartus shown in Fig. 1. The sieve over the funnel was 10 mesh for No. 13 and 30 mesh for the other samples. The height of the lower end of the funnel was fixed to be 35 mm from a horizontal plate. When the vertex of a cone formed with powder reached at the lower end of the funnel, the dropping of powder was stopped and then, the diameters of the cone-base, $\bar{l}$ mm, were measured at two orthogonal directions. The angle of repose, θ, was calculated from the mean diameter $\bar{l}$ with Eq. 1.

$$\theta = \tan^{-1}(2 \times 35/\bar{l}) \qquad \text{Eq. 1}$$

The angles were measured 5 times on a sample and the average value was used.

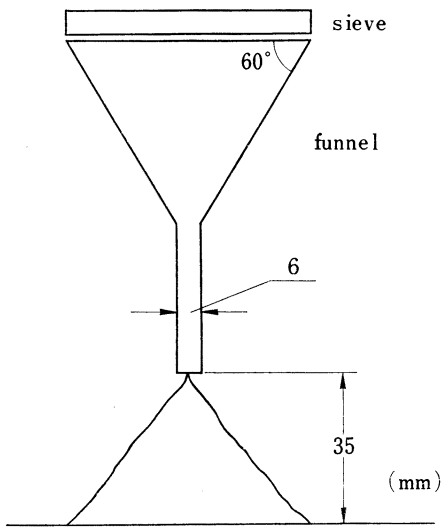

Fig. 1. Apparatus for Determining Angle of Repose

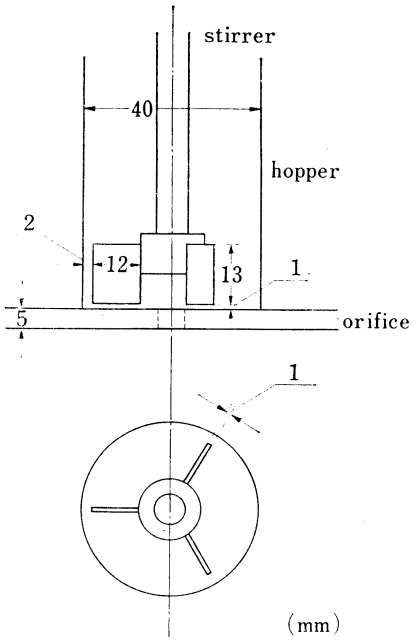

Fig. 2. Apparatus for Flow-Test

The tests of flow in orifices were done with the apparatus shown in Fig. 2. In order to avoid large variation of the experimental values for the powders of bad fluidity, owing to the fluctuations of bridge-formation in orifices, the powder-bed in the hopper was being stirred by a rotor with three blades and the rotor-speed of 3.87 rpm. A vibration-method was also tried but it only facilitated the blockade of orifices for some kinds of powders and therefore, the stirring-method was selected. Ten kinds of orifices were used and their diameters were from 1 mm to 10 mm at intervals of 1 mm. The weight of the sample discharged through an orifice was measured with a transducer connected to an electronic recorder and a mass-flow-rate was determined from a chart of the recorder.

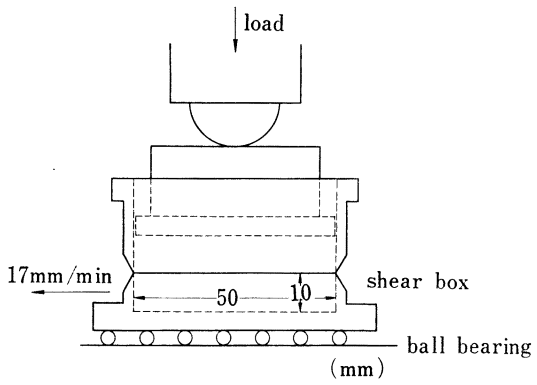

Fig. 3. Diagram of Shearing Cell

A sketch of the apparatus for shear-tests is shown in Fig. 3. Shear-box was filled with such amount of sample as, after a preliminary compaction for 1 min under a constant pressure, the distance between the shear-plane and the upper surface of the sample would be about 1 cm. After the preliminary compaction, a shear-test was done under a lower range of pressure than that of the compaction. The pressure was applied with a lever and load. A sample was compacted preliminarily under three different pressures ranging from 184 to 3880 g/cm^2. And the compacted samples were sheared under 2 pressures as low as possible; 25 and 114 g/cm^2. The apparent density of the compacted sample was determined from its thickness and weight. The shear-force and the horizontal displacement of the lower cell were measured with a load-

cell and a differential transformer, respectively. The shear-force was determined from the height of the first peak in a shear-pattern. The measurements were repeated under the same conditions and the average value was used.

Result

Discharge from Orifices

A discharge-rate Q was expressed as a volume-rate (cm^3/min) and determined by dividing the mass-flow-rate by ρ_a. It was considered that not the cross-sectional area of an orifice itself but its relative dimension to a particle is a governing factor of the discharge-rate. Therefore, the relation between Q and $(\phi/dp)^2$, ϕ being an orifice-diameter, was determined and shown in Fig. 4. Thus Eq. 2 was derived.

$$Q = a((\phi/dp)^2-(\phi_0/dp)^2) \qquad \text{Eq. 2}$$

a and $(\phi_0/dp)^2$ for each sample are shown in Table II.

TABLE II. The Slope (a) and the Intercept $(\phi_0/dp)^2$ of Q vs. $(\phi/dp)^2$ Plot and Angle of Repose

Sample No.	a (cm^3/min)	$(\phi_0/dp)^2$ (—)	ϕ_0[a] (cm)	θ (°)
1	—	—	1.0[b]	57
2	—	33×10^4[c]	0.7[b]	49
3	27×10^{-4}	53×10^2	0.30	40
4	57×10^{-4}	58×10	0.10	37
5	14×10^{-2}	20×10	0.17	36
6	52×10^{-3}	25×10	0.14	37
7	18×10^{-3}	36×10	0.12	38
8	11×10^{-2}	25×10	0.20	40
9	25×10^{-3}	11×10^2	0.30	43
10	67×10^{-4}	27×10^2	0.35	45
11	88×10^{-5}	12×10^3	0.62	48
12	25×10^{-4}	52×10^2	0.36	42
13	26×10^{-1}	21	0.27	36
14	13×10^{-2}	20×10	0.17	36
15	—	—	1.0[b]	54
16	—	29×10^4[c]	0.7[b]	51
17	11×10^{-5}	58×10^3	0.55	33
18	19×10^{-5}	25×10^3	0.37	31
19	21×10^{-3}	20×10	0.07	24
20	—	—	1.0[b]	42

a) calculated from $(\phi_0/dp)^2$ b) observed c) calculated from ϕ_0 observed

ϕ_0 seems to be the minimum-orifice-diameter necessary for powder to flow out. No. 2 and No. 16, whose ϕ_0 is shown to be 7 mm in Table II, discharged from the orifices of 7 mm-, 8 mm-, 9 mm-, and 10 mm-diameter but the discharge-rates were too small to determine the a. Therefore, the diameter of the orifice at which the discharge began, 7 mm, was shown as ϕ_0 on them. On No. 1, No. 15 and No. 20, discharge did not take place even at the orifice of 10 mm-diameter. The angles of repose are also shown in Table II.

Shear-Test

The representative shear-patterns of irregular and spherical particles are shown in Fig. 5 and Fig. 6, respectively (The scale of the ordinate is arbitrary on each sample). These indicate that the patterns of the spherical particles, except for No. 20, were pulse-like and

different from those of the irregular ones, while these specific pulse-patterns disappeared in No. 16 and No. 18 when magnesium stearate was added to No. 15 and No. 17, respectively.[6]

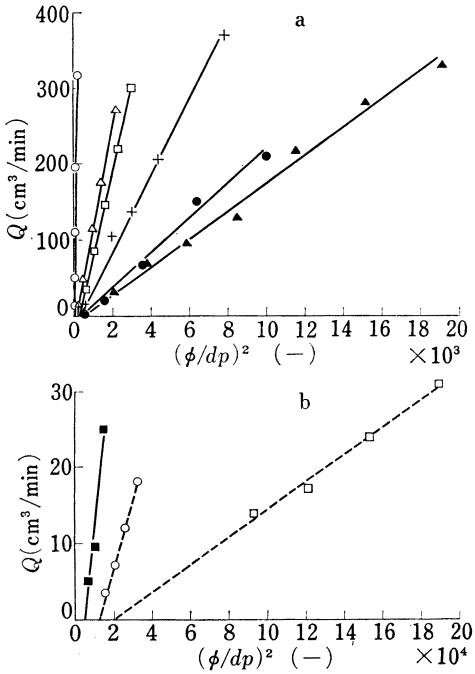

Fig. 4. Relation between Discharge Rate and the Relative Orifice-Area to a Particle

—+—: No. 6, —▲—: No. 7, —□—: No. 8,
---○---: No. 11, —■—: No. 12, —○—: No. 13,
—△—: No. 14, ---□---: No. 18, —●—: No. 19

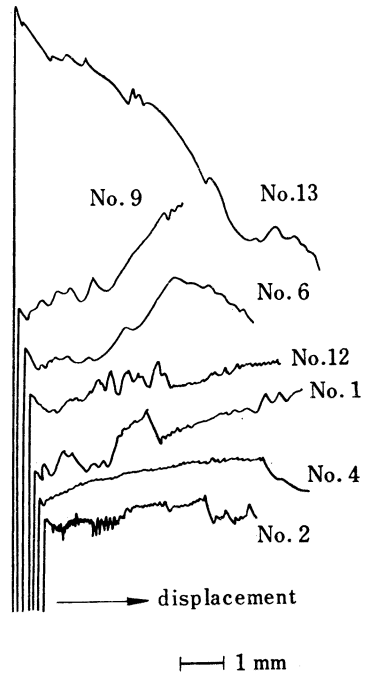

Fig. 5. Shear Patterns of Irregular Particles

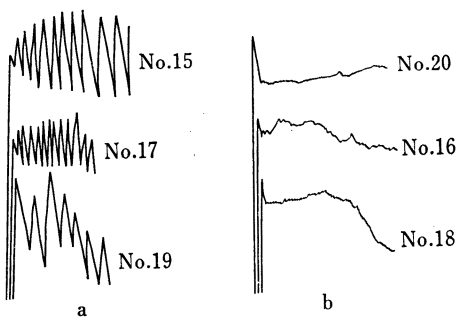

Fig. 6. Shear Patterns of Spherical Particles

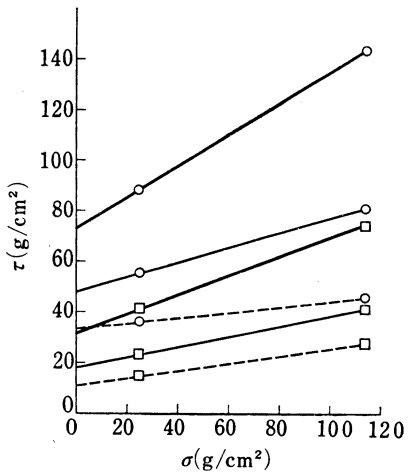

Fig. 7. Shear Tests of Powders Compacted preliminarily under Different Pressures

□: No. 11 ○: No. 20
——: P=930 g/cm² ——: P=370 g/cm²
- - - - - - - : P=185 g/cm²

6) This will be discussed in a separate paper.

Fig. 7 shows some relations between the normal stress σ (g/cm^2) and the shear stress τ (g/cm^2) which was determined from the height of the first peak in the shear-pattern. On the basis of the assumption that the Coulomb equation, Eq. 3, held for in each pressure of the preliminary compaction, P (g/cm^2), μ_i and C were determined.

$$\tau = \sigma\mu_i + C \qquad \text{Eq. 3}$$

μ_i: interparticle frictional coefficient (−)
C: interparticle cohesion (g/cm^2)

Discussion

Interparticle Cohesion

The interparticle cohesion per unit area, C(g/cm^2), for each compaction-pressure P was determined by using Eq. 3. An interparticle cohesion at point of contact, F(g), was calculated from C by using the Rumpf equation,[7] Eq. 4.

$$F = 8/9 \times \pi d p^2 C/k(1-\varepsilon) \qquad \text{Eq. 4}$$

The compaction-force p applied at point of contact must be determined in order to find the effect of the compaction-pressure on F. The Rumpf equation seems unsuitable to be used in order to determine p from P, because the absorption of forces at the powder-wall interface takes place along the vertical direction and the pressure-distribution is anisotropic in a powder-bed. However, it was considered that a relative value of p could be determined by using the Rumpf equation. p was calculated by using Eq. 5.

$$p = 8/9 \times \pi d p^2 P/k(1-\varepsilon) \qquad \text{Eq. 5}$$

Rumpf has proposed eq. 6 as the relation between co-ordination number k and fractional voidage ε.

$$k\varepsilon = \pi \qquad \text{Eq. 6}$$

However,[8] Ridgway has pointed out that Eq. 6 dose not hold for large ε and has proposed Eq. 7.

$$\varepsilon = 1.072 - 0.1193k + 0.00431k^2 \qquad \text{Eq. 7}$$

The results of calculations indicate that the difference between k obtained from Eq. 6 and that from Eq. 7 is significant in the larger ε than about 0.5. Therefore, in this paper k was calculated from Eq. 6 for $\varepsilon < 0.5$ and from Eq. 7 for $\varepsilon \geqq 0.5$. The fractional voidage ε was determined from apparent density of a powder-bed in the shear-cell and the particle density. Fig. 8 shows the relations between p and F on some samples. Two types are found in this relation; in some samples F decreases with p and in the other samples F is independent of p and nearly constant. The interparticle cohesion at point of contact, F_0, corresponding to the state of powders without external forces, was determined by extrapolating p to zero on the basis of the assumption of linear relations between p and F. F_0 values are shown for all samples

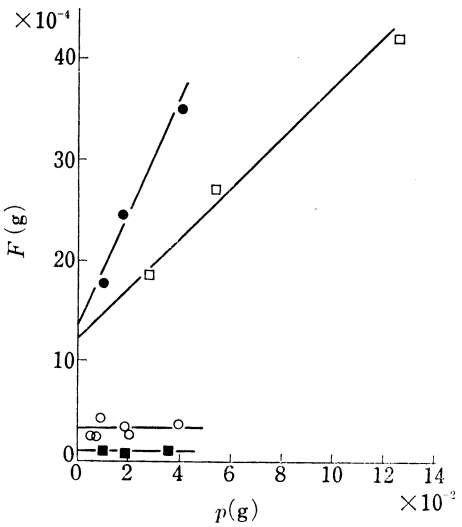

Fig. 8. Relation between Interparticle Cohesion and Compaction-Force at Point of Contact

—■—: No. 4 —□—: No. 11
—○—: No. 12 —●—: No. 20

7) H. Rumpf, "Agglomeration," ed. by W.A. Knepper, Willey, 1961, p. 379.
8) K. Ridgway and K.J. Tarbuck, *Brit. Chem. Engg.*, **12**, 384 (1967).

TABLE III. Interparticle Cohesion at Point of Contact and Particle Weight

Sample No.	Fo (g)	ρpdp^3 (g)	$Fo/\rho pdp^3 \times 10^{-2}$ (−)	Dependency of F on p
1	23×10^{-6}	26×10^{-10}	88	dependent
2	15×10^{-6}	26×10^{-10}	58	dependent
3	16×10^{-5}	10×10^{-8}	16	independent
4	8×10^{-5}	10×10^{-8}	8.0	independent
5	11×10^{-4}	31×10^{-7}	3.5	independent
6	63×10^{-5}	11×10^{-7}	5.6	independent
7	35×10^{-5}	42×10^{-8}	8.3	independent
8	70×10^{-4}	32×10^{-7}	22	dependent
9	40×10^{-4}	11×10^{-7}	35	dependent
10	25×10^{-4}	49×10^{-8}	51	dependent
11	13×10^{-4}	23×10^{-8}	57	dependent
12	30×10^{-5}	18×10^{-8}	17	independent
13	37×10^{-3}	24×10^{-5}	1.6	independent
14	10×10^{-4}	24×10^{-7}	4.2	dependent
15	19×10^{-6}	33×10^{-10}	58	independent
16	22×10^{-6}	33×10^{-10}	67	independent
17	34×10^{-6}	81×10^{-9}	19	dependent
18	27×10^{-6}	18×10^{-9}	15	dependent
19	0.0	30×10^{-8}	0.0	dependent
20	14×10^{-4}	29×10^{-8}	48	dependent

in Table III. Although the equations used for the determination of F_0 have been derived on spherical and mono-dispersed particles, some samples used in this experiment are nonspherical and/or not considered to be mono-dispersed. In spite of it, the interparticle cohesions determined in this experiment were almost in the same order (10^{-6}—10^{-3}g) as of the values determined by Arakawa, *et al.* on white alundum[3b] (see Fig. 9) and glass beads surface-treated with silver or hexamethyl disilazane.[9] Therefore, it is considered that the errors caused by using these equations in the calculation of the interparticle cohesion were not so large in this experiment.

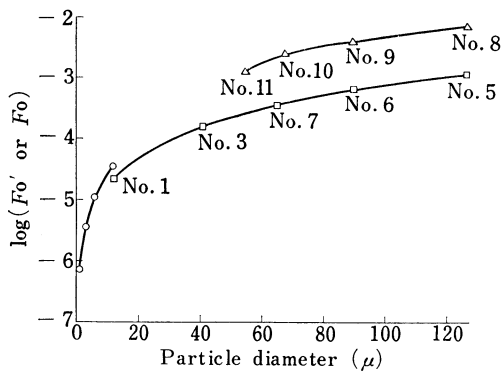

Fig. 9. Relation between Interparticle Cohesion and Particle Diameter

—□—: lactose
—△—: crystalline cellulose
—○—: white alundum (Arakawa's data)

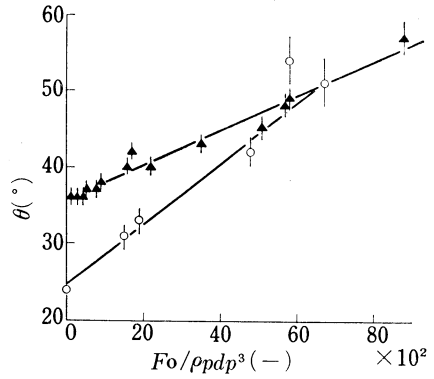

Fig. 10. Relation between Angle of Repose and the Ratio of Interparticle Cohesion to Particle Weight for a Particle

—○—: spherical particle
—▲—: irregular particle

9) M. Nishino and M. Arakawa, The 9th Symposium on Powder Science, Toyama, Oct. 1971.

It is considered that if interparticle distances were changed irreversibly or plastic deformations were occured with change of the contact areas by loading, the interparticle cohesion at point of contact, F_0, corresponding to that under zero compacting pressure, must be determined by extrapolating to $p=0$ in the plots of F against p, (F is an interparticle cohesion at point of contact for a compacting force p). The plots of F_0 against particle-diameters are shown in Fig. 9, together with the findings (F_0') for white alundum by Arakawa, *et al.*[3b] This figure indicates that the interparticle cohesion at point of contact increases monotonically with the particle-diameter. Although not shown here, μ_t determined on every sample was smaller than 1.0, and therefore the frictional force due to particle-weight was 10^{-4}—10^{-2} times as large as F_0 shown in Table III. This finding suggests that the contribution of the frictional force to the interparticle interaction is neglesible under the conditions of no loads.

Angle of Repose

It was considered, on the angle of repose of a pile formed naturally, that particle-weight is a driving force for downward motion and the interparticle cohesion F_0 is a inhibiting factor for the motion. In order to examine the influence of particle-weight or F_0 on the angle of repose, they were plotted against the angle of repose. No correlations, however, were recognized between them. Moreover, the angle of repose was plotted against the ratio of interparticle cohesion F_0 to particle-weight, namely against $F_0/\rho pdp^3$, and the plots are shown in Fig. 10. In Fig. 10, the length of a vertical line drawn for each plot represents the variation-range of θ. From these results, eq. 8 was derived.

$$\theta - \theta_0 = \alpha F_0/\rho pdp^3 \qquad \text{Eq. 8}$$

The constants, θ_0 and α, depend on the particle-shape which is spherical or irregular. The following values were determined: spherical partcles; $\theta_0=25.0°$ and $\alpha=4.0\times10^{-3}$, irregular particles; $\theta_0=35.5°$ and $\alpha=2.3\times10^{-3}$.

Discharge-Rate

The relation between the slope a and the intercept $(\phi_0/dp)^2$ in the plots of Q *vs.* $(\phi/dp)^2$ showed linearity with a slope of -1 in logarithmic plots as shown in Fig. 11; namely, a was inversely proportional to $(\phi_0/dp)^2$. From the findings presented above, it can be seen that the minimum orifice-diameter necessary for discharge of powder is closely related with the ratio of the increment of the discharge-rate to that of the cross-sectional area of the orifice.

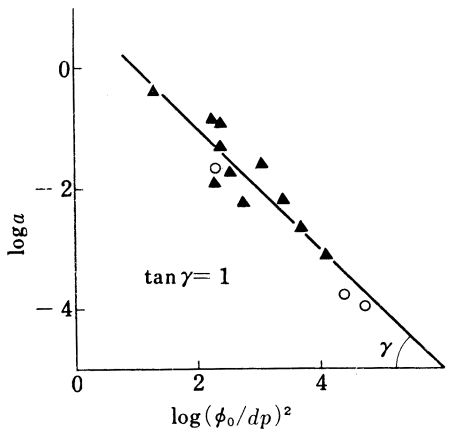

Fig. 11. Relation between the Slope and the Intercept in the $(\phi/\mathrm{dp})^2$ Co-ordinate of Q vs. $(\phi/\mathrm{dp})^2$ Plot

○: spherical particle
▲: irregular particle

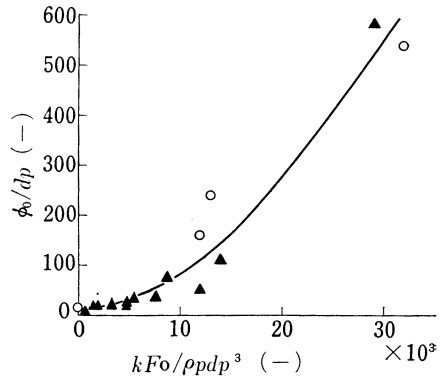

Fig. 12. Relation between the Relative Dimension of the Minimum Orifice Diameter to a Particle and the Ratio of Cohesion Force to Gravitational Force for a Particle

○: spherical particle
▲: irregular particle

As in the case of the angle of repose, the relation between ϕ_0/dp and $F_0/\rho p dp^3$ was examined but a good correlation was not found between them. Now upon this, co-ordination number k, which is the number of contact-points per one particle in a powder-bed, was taken into account and the relation between ϕ_0/dp and $kF_0/\rho p dp^3$ was determined as shown in Fig. 12, which indicates a good correlation between them. F_0 is the interparticle cohesion under zero compacting pressure and therefore k was determined as the co-ordination number in a loose pile formed naturally, namely from ρa and ρp by using Eq. 6 and 7. ϕ_0/dp, k and $kF_0/\rho p dp^3$ for each sample are shown in Table IV.

TABLE IV. Relative Dimension of the Minimum Orifice Diameter to a Particle, Co-ordination Number and Ratio of Cohesion Force to Gravitaftional Force for a Particle

Sample No.	ϕ_0/dp (—)	k (—)	$kFo/\rho p dp^3 \times 10^{-3}$ (—)
1	—	4.13	36
2	580	4.94	29
3	73	5.47	8.8
4	24	7.06	5.6
5	14	5.97	2.1
6	16	5.83	3.3
7	19	5.76	4.8
8	16	2.13	4.7
9	33	2.22	7.8
10	52	2.27	12
11	110	2.37	14
12	72	5.00	9
13	4.6	5.27	0.84
14	14	4.80	2.0
15	—	4.01	23
16	540	4.80	32
17	240	6.69	13
18	160	8.05	12
19	14	7.48	0
20	—	3.84	18

Relation between Angle of Repose and Discharge Behavior

The discharge-rate is expressed by Eq. 2 and its coefficients, a and $(\phi_0/dp)^2$, can be interrelated as in Eq. 9.

$$a \fallingdotseq \beta(\phi_0/dp)^{-2} \qquad \text{Eq. 9}$$

β: constant

In view of these findings, the discharge-rate may be considered to be determined by ϕ_0/dp. And ϕ_0/dp is represented by Eq. 10 on the basis of the monotonic relation shown in Fig. 12, (the function was not determined).

$$\phi_0/dp = f(kF_0/\rho p dp^3) \qquad \text{Eq. 10}$$

Eq. 11 is derived from Eq. 8 concerning the angle of repose.

$$F_0/\rho p dp^3 = (\theta - \theta_0)/\alpha \qquad \text{Eq. 11}$$

Eq. 12 is derived by substituting eq. 11 into Eq. 10.

$$\phi_0/dp = f(k(\theta - \theta_0)/\alpha) \qquad \text{Eq. 12}$$

ϕ_0/dp is plotted against $k(\theta - \theta_0)/\alpha$ in Fig. 13. Thus, when the co-ordination number k was taken into account, a distinct correlation could be obtained between the behavior of discharge and the angle of repose.

Both ϕ_0/dp and θ are closely related with $F_0/\rho pdp^3$ which is determined from the particle-weight and the interparticle cohesion. For ϕ_0/dp, however, the co-ordination number k must be taken into account, while for the angle of repose the particle-shape, which is spherical or irregular, must be taken into account. From these facts, it can be seen that the discharge-behavior is greatly affected by the co-ordination number, namely by the interaction between particles in the powder-bed, as well as by $F_0/\rho pdp^3$ and hardly affected by the particle-shape, whereas the angle of repose is barely dependent on the co-ordination number and greatly affected by the particle-shape; the roll and the slip of particles on the powder-surface may be predominant factors governing the angle of repose.

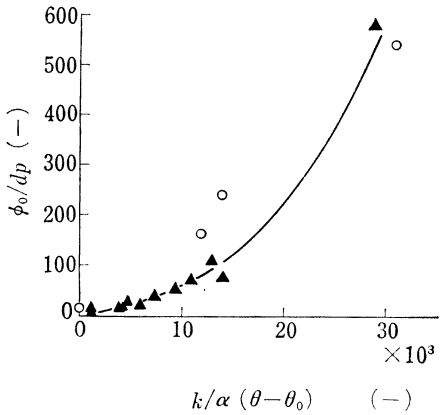

Fig. 13. Relation between the Relative Dimension of the Minimum Orifice Diameter to a Particle and Angle of Repose

○: spherical particle
▲: irregular particle

Acknowledgement The authors wish to express their appreciation to Professor H. Kuno of Keio University for his valuable discussion and to thank Dr. H. Negoro of director of this laboratory for permission for publication of this paper and Dr. T. Morioka for his encouragement.